Shahrood University of Technology
Iranian Society of Mining Engineering (IRSME)
Journal of Mining and Environment (JME)
journal homepage: www.jme.shahroodut.ac.ir
THOMSON REUTERS

# Modeling of Induced Polarization and Resistivity Data for Prospecting and Exploration of Polymetallic Deposit in Kaboudan Area, East of Iran

Farzaneh Jamali, Ali Reza Arab Amiri*, Abolghasem Kamkar Rouhani and Ali Bahrami

*Faculty of Mining, Petroleum and Geophysics Engineering, Shahrood University of Technology, Shahrood, Iran*

***Article Info***

*Received 12 December 2020*
*Received in Revised form 16 May 2021*
*Accepted 11 June 2021*
*Published online 11 June 2021*

*DOI:10.22044/jme.2021.10353.1985*

***Keywords***

*Induced polarization*
*Electrical resistivity*
*Polymetallic deposits*
*3D modeling*
*Rectangle array*

***Abstract***

In any geophysical exploration, the final goal is to achieve an accurate image of the relevant underground property. In order to achieve this, the geophysical operation using the electrical resistivity and induced polarization (IP) methods is conducted to explore the sub-surface sulfide mineralization. Considering the mineralization evidence in the Kaboudan area near the Bardeskan city, first, geophysical surveying of the polymetallic deposit is carried out using the electrical resistivity and IP methods by employing the rectangle array in order to detect the electrical anomalies in the area. Then for delineation of the identified anomalies and investigation of the mineralization in the area, the 2D resistivity and chargeability cross-sections are prepared and interpreted with the help of the geological information. This geophysical survey in the area has led to the identification of several potential areas for mineralization. Then in order to obtain a detailed picture of the sub-surface mineralization and an overview of the in-depth mineralization distribution, a 3D modeling of the acquired data is made, and the results of this modeling are shown in 3D forms. The mineralization zones are identified in the studied area from their high chargeability values as well as the low to medium electrical resistivity amounts. This can be attributed to the metal mineralization and the presence of sulfide minerals in the mineralization zones. Mineralization in many places of the studied area is determined with an approximate east-west trend as well as somewhat varying the intensities of the electrical resistivity and chargeability amounts. The geological and drilling information obtained from the area confirm the interpretations.

## 1. Introduction

The studied area is located in the Kaboudan area, 270 km SW of Mashhad and north of Bardeskan. This area is part of the Central Iran zone and the central zone of the Alpine-Himalayan belt [25]. The mineralization in this area is of massive sulfide mineralization type [25]. The mineralization evidence and outcrops such as the copper sulfides, silica-feldspar, and dome-shaped shear units have been found in the area. Also there are diabetic dykes in parts of the area [23; 25]. With this evidence, this area is a good target for further investigation.

The geophysical techniques rely on the changes in the physical properties of minerals or the rocks that enclose them to show the mineralization zone directly or indirectly. The physical response could be direct (due to some of the properties of the rock such as density, natural radioactivity, magnetic properties, and resistivity) or indirect (a reaction due to being exposed to a physical stimulus). The geophysical methods have made a very little damage to the environment, and are more economical than the test excavations. Through the valuable information obtained from a geophysical survey, a more efficient and effective drilling and excavation program can be planned, which provides us with the site information without the need for excavation [26]. Therefore, the best option is to use several different geophysical methods simultaneously, thus identifying a specific physical

*Corresponding author: alirezaarabamiri@yahoo.com (A. R. Arab Amiri).*

and/or structural feature of the sub-surface through each method. In this way, a specific area can be surveyed with two or more geophysical methods, so by combining and comparing the results obtained, we can have a more complete and accurate picture of the sub-surface [4].

The electrical resistivity and induced polarization (IP) methods are among the most important geophysical methods used to identify and explore the potential areas for sulfide mineralization. The resistivity images can be explored for resistivity contrasts, which can be indicative of lithological changes. On that account, the electrical resistivity method can be used in order to identify the 2D and 3D distributions of electrical resistivity (or its inverse that is electrical conductivity [6]. This feature, which in the IP parameter method is related to the petro-physical properties of rocks and has little effect on their electrical resistivity, is the most important advantage of this method over the resistivity method. This makes it possible to evaluate the relevant properties of rocks such as the volumetric content of electronically conductive mineral grains, their dominant sizes, the dominant sizes of pores or grains of dielectrics, clay content, and filtration coefficient [11]. Due to the high success of the IP method in investigation of the low-grade ore deposits such as disseminated sulfides, this method is widely used in the exploration of base metals. These sediments have a low conductivity, and therefore, are not easily detectable by the electrical resistivity (and electromagnetic) methods but fortunately, they have strong IP effects. Thus IP is by far the most effective geophysical method that can be used in the search for such targets [15].

The two methods of electrical resistivity and IP have been widely used in the mineral exploration and geological studies [8; 12; 19; 22]. The IP method has a very long history in geophysics. This method has been used for many years in a variety of applications such as mining [20; 10], hydrogeology [13; 16; 1], geological studies [6; 21], mapping contaminated plumes [7; 3], exploration of buried pipes [28], and hydrocarbon studies [29].

In order to use the geophysical methods, it is necessary that there is a difference in the physical properties (magnetism, susceptibility, density, electrical resistivity, seismic velocities, etc.) of soils and rocks. The geophysical methods complete with each other because they are sensitive to different physical parameters [17]. The purpose of this research work is to investigate and explore the polymetallic deposit in the Kaboudan area using an integration of the electrical resistivity and IP methods. In order to provide a good picture of the sub-surface and to gain an overview of the area, the promising zones in the area were identified using the electrical resistivity and IP data acquired by the rectangle array. Then these promising zones were investigated using the electrical resistivity and IP data acquired by the dipole-dipole array. In order to obtain a more accurate and reliable picture of the sub-surface, the collected electrical resistivity and IP data was also modeled using the dipole-dipole array, and the results obtained were displayed. Finally, the results of modeling and interpretation of the electrical resistivity and IP data were compared with the results of the drilling made in the area.

## 2. Studied area

Kaboudan is a village in the central district of the Bardeskan County, which is located in SW of the Khorasan-e-Razavi Province. Figure 1 shows the access road to the studied area as well as the location and topography of the area. The Kaboudan area is one of sixteen sheets of 1:100,000 geological sheet of the Bardeskan region. The studied area is included in this geological sheet [27]. Figure 2 shows the location and also the geological map of the studied area. The silica-feldspar and dome-shaped shear units with high silica content have outcrops in the area [25]. The Taknar Formation is a remnant of an infertile continent rift that is attributed to Precambrian [24]. The Taknar Formation has been exposed to low-grade metamorphism (green schist facies) [14]. In general, mineralization has occurred in the area of contact of acid metatrophies and metariolites with evolved green schists. Diabasic dykes appear to have played an appropriate thermal role in the formation of the siliceous-feldspar sheets in the rhyolitic domes. This zone is relatively large, and includes a variety of volcanic-sedimentary-stratigraphic bands (bulk sulfide). Iron mineralization in the area has taken place in the upper part, and the oxide-argillic-limonite-stochastic alteration (quartz-sericite schist filled with oxide) in the lower part. The mineralization evidence has been found in malachite, magnetite, manganese, and iron and copper sulfides [23]. However, the ore deposit in the Taknar Formation is distinguished from the other masses of sulfide due to the presence of more than 60% magnetite with sulfide minerals. The Taknar polymetallic deposit has been introduced as a magnetite rich Taknar type polymetallic (Cu-Zn-Au-Ag-Pb)

sulfide deposit [14]. Its rocks are mostly green schists and rhyolite metatopes and siliceous-feldspar sheets. Diabetic dykes have also been found in parts of the area. The mineralization zone in the form of magnetite, malachite, and pyrite and chalcopyrite sulfides coincides with the chlorite and hematite-limonite alterations, and stochastic alterations [23].

## 3. Methodology, results, and discussion

The geophysical methods are useful and practical for obtaining a model of sub-surface structures as well as the information about the lithology and physical parameters of the earth [17]. A major advantage of the geophysical methods is that they can be used in order to explore great depths of several hundred meters (and in some, cases several kilometers), while these depths are less accessible for the geochemical and geological surveys [26]. In the electrical resistivity surveys, the aim is to determine the sub-surface resistivity distributions by taking measurements of the apparent resistivity on the ground surface. Obtaining the true resistivity from this data is done by performing an inversion of the observed apparent resistivity values and importing anomalous or heterogeneous conditions [2]. The availability of the 2D, and later, 3D inversion programs for the resistivity and IP data made it possible to interpret this data faster and more accurately [30].

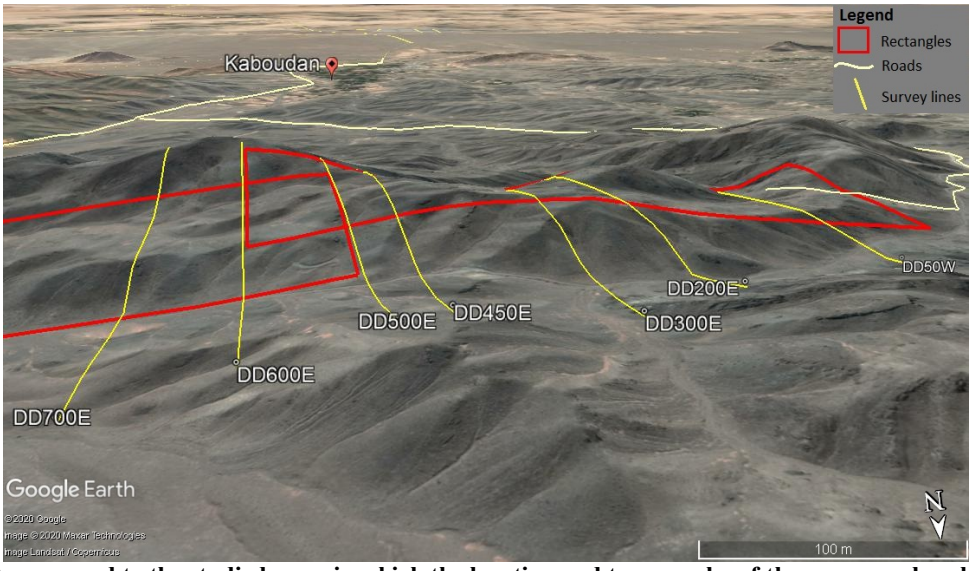


**Figure 1. Access road to the studied area, in which the location and topography of the area are also observed [9].**

The sub-surface structures are naturally three-dimensional. Hence, for a more accurate and reliable study, it is better to use a 3D geo-electrical resistivity survey with a 3D interpretation model, especially in the subtle heterogeneous subsurface. The studies show that the 3D geo-electrical resistivity images are superior to the 2D resistivity images. Consequently, the 3D geo-electrical resistivity imaging is a more appropriate and a better method for an accurate mapping of the sub-surface and spatial distribution of the electrical conductivity and petro-physical properties [2].

In order to characterize the lateral variations and distribution of the anomalous bodies, the geophysical resistivity and IP prospecting was carried out using 3 rectangle arrays with the distance of current electrodes (AB) equal to 800 m, the distance between the consecutive lines being equal to 50 m, and the distance between the consecutive stations or geophysical measurements being equal to 20 m. Then for the in-depth investigations on the specified areas, a dipole-dipole array was used. Due to the low EM coupling between the current and potential circuits, this array is widely used in the resistivity and IP surveys. According to the previous studies and information (such as trenches) as well as the results of the survey with a rectangular array, the resistivity and IP data along seven survey lines with distances of 100 to 150 m and AB of 20 m and 40 m were also carried out, and the quantities of chargeability and the apparent electrical resistivity were measured.

The Res2Dinv and res3Dinv softwares were used to model the data. These programs use the smoothness-constrained Gauss-Newton least-squares inversion technique in order to automatically produce a 2D/3D model of the sub-

surface from the apparent resistivity data without any need for providing a starting model. It supports the Wenner, Schlumberger, pole-pole, pole-dipole, dipole-dipole, multiple gradient and non-conventional arrays. The inversion routine used by these program is based on the smoothness constrained least-squares method, which is based on the following equation [18]:

$$(J^TJ + uF)d = J^tg \quad (1)$$

where $F = f_xf_x^T + f_zf_z^T$, $f_x$ = horizontal flatness filter, $f_z$ = vertical flatness filter, J = matrix of partial derivatives, u = damping factor, d = model perturbation vector, and g = discrepancy vector.

The output model of these softwares is shown with the RMS error, in which the root-mean-square (RMS) error quantifies the difference between the measured resistivity values and the values calculated from the true resistivity model. However, a model with the lowest possible RMS error geologically may not always be the best model, and it can sometimes show unrealistic and larger changes in the model resistivity values. In general, the best method for selecting a model is the one that does not change the RMS error significantly.

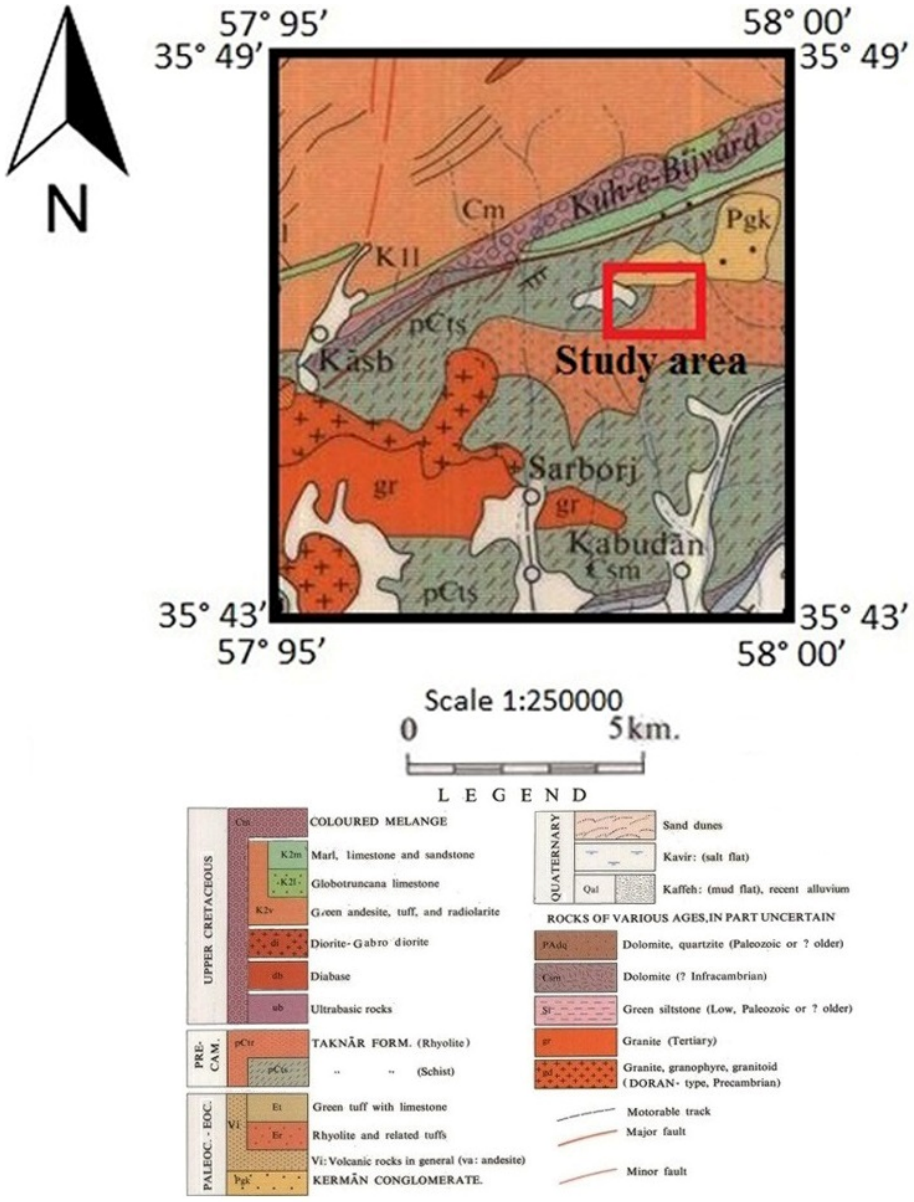


**Figure 2. Geological map of the studied area [5].**

### 3.1. Electrical prospecting of studied area using rectangle array

The contour-maps of the collected electrical resistivity and IP data using the rectangle array were plotted, and the regions with a high chargeability and a low to medium resistivity were specified as the promising regions in the plotted contour-map. Figures 3 and 4 show the results of the plotted resistivity and IP data using this array, in which three promising areas can be identified.

According to Figure 3, the high chargeability areas having an east-west approximate trend were identified as the promising areas. According to Figure 4, these areas correspond to the areas of low to moderate electrical resistivity. The areas of low electrical resistivity, which are mainly in the north and northeast of this area, correspond to the green schists, and the areas of high electrical resistivity, mainly in the south, also correspond to the acidic metatuff and metariolites.

Based on the findings and evidence of mainly sulfide mineralization in the form of magnetite, malachite and pyrite, and chalcopyrite, the identified areas are the most promising areas for mineralization. In total, three promising areas were identified, and seven survey lines were designed on these areas. Then on the designed survey lines, we studied the changes and expansion of the anomalies in-depth, and obtained the IP and electrical resistivity data using the dipole-dipole array.

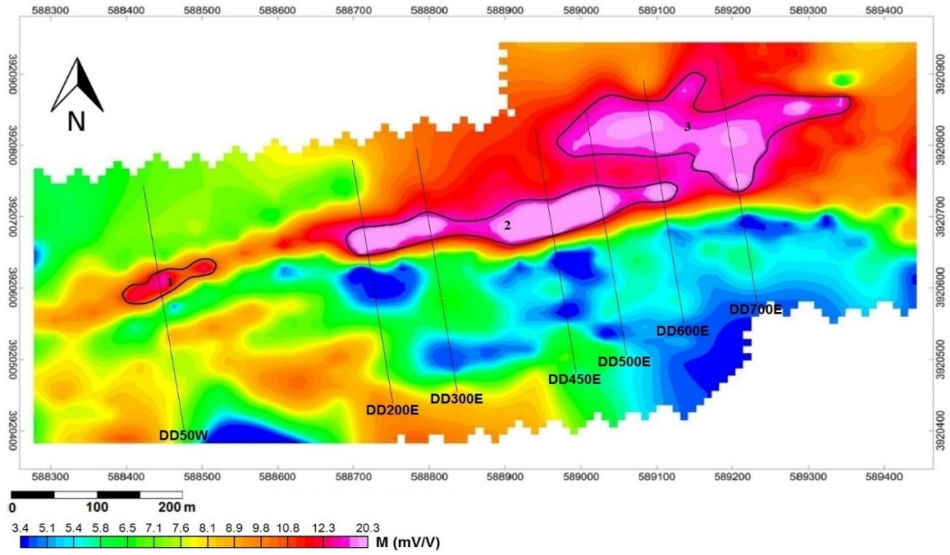


**Figure 3. Contour-map of the IP data obtained using the rectangle array.**

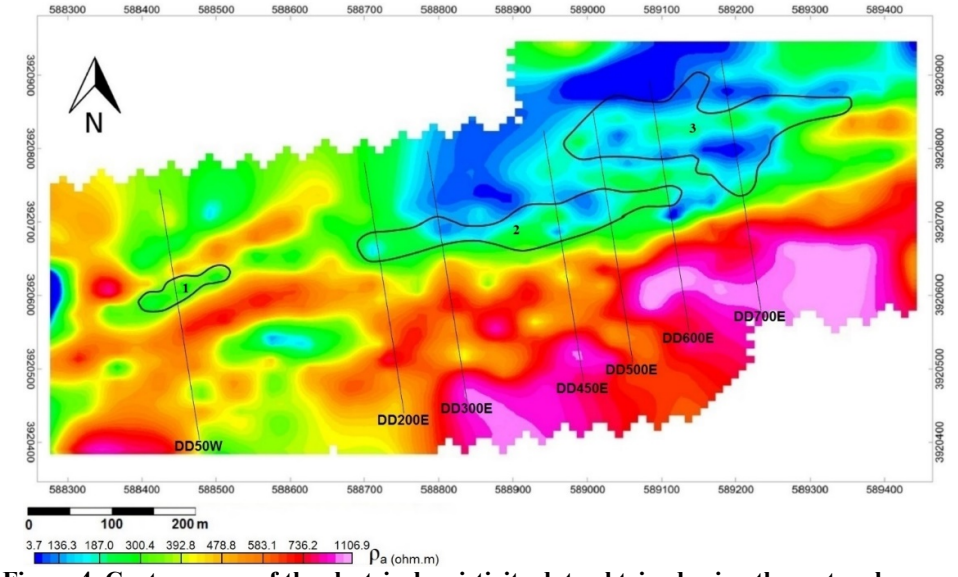


**Figure 4. Contour-map of the electrical resistivity data obtained using the rectangle array.**

### 3.2. 2D resistivity and IP modeling

As shown in Figures 3 and 4, three promising areas were identified, in which seven survey lines were designed for the resistivity and IP measurements using the dipole-dipole array. On the promising area 1, a survey line, on the promising area 2, four survey lines, and on the promising area 3, two survey lines were considered for the measurements. The drilling operations were also carried out on a number of survey lines. Table 1 shows the information obtained from these drilling operations.

**Table 1. Drilling operations performed in the studied area.**

| Survey line | Station (m) | Drilling | Azimuth (degrees) | Slope (degrees) | Depth (m) |
|---|---|---|---|---|---|
| DD50W | 220 | PBH1 | 172 | 20 | 80 |
| DD200E | 230 | PBH2 | 172 | 25 | 80 |
| DD450E | 220 | PBH3 | 172 | 20 | 100 |

The resistivity and IP measurements were made along the survey line DD50W using the dipole-dipole array with the electrode separations of 20 m and 40 m and steps of 20 m in order to investigate the sub-surface anomalies at the promising area 1. Figures 5 and 6 show the pseudo-sections and section of resistivity and IP of inverse modeling of the profile DD50W and the RMS error and iteration number for each model. Figure 7 demonstrates the results of the inverse modeling of the resistivity and IP data along the survey line DD50W by applying the topographic correction on the survey line. As it can be seen in Figure 7, an anomaly with a high chargeability is observed at stations between 180 m and 220 m and approximately up to 40 m below the ground level that corresponds to the areas with a low electrical resistivity. Furthermore, the presence of Fe and Cu sulfides in this area may be a reason for the anomaly of sulfide mineralization.

Drilling in this area shows both types of massive and disseminated sulfide mineralization that confirms the results obtained from the geophysical interpretations, and the mineralization zones well-coincide with the anomaly areas in the chargeability and electrical resistivity cross-sections.

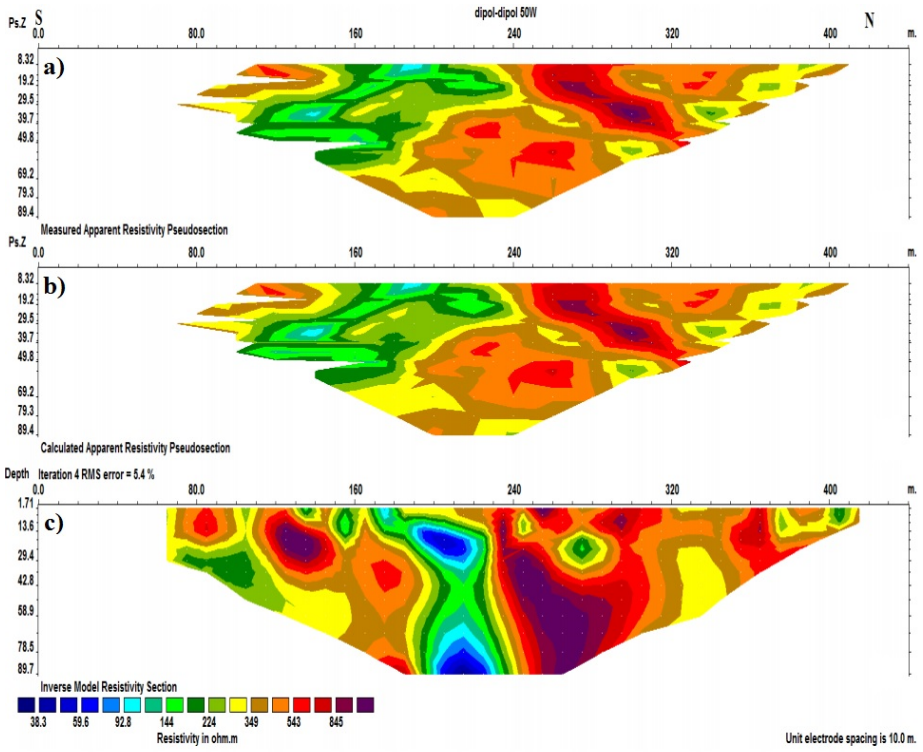


**Figure 5. Pseudo-sections and section of resistivity of inverse modeling of profile DD50W a) Pseudo-section of the measured data, b) Pseudo-section of the calculated data, c) Section of the inverse modeling.**

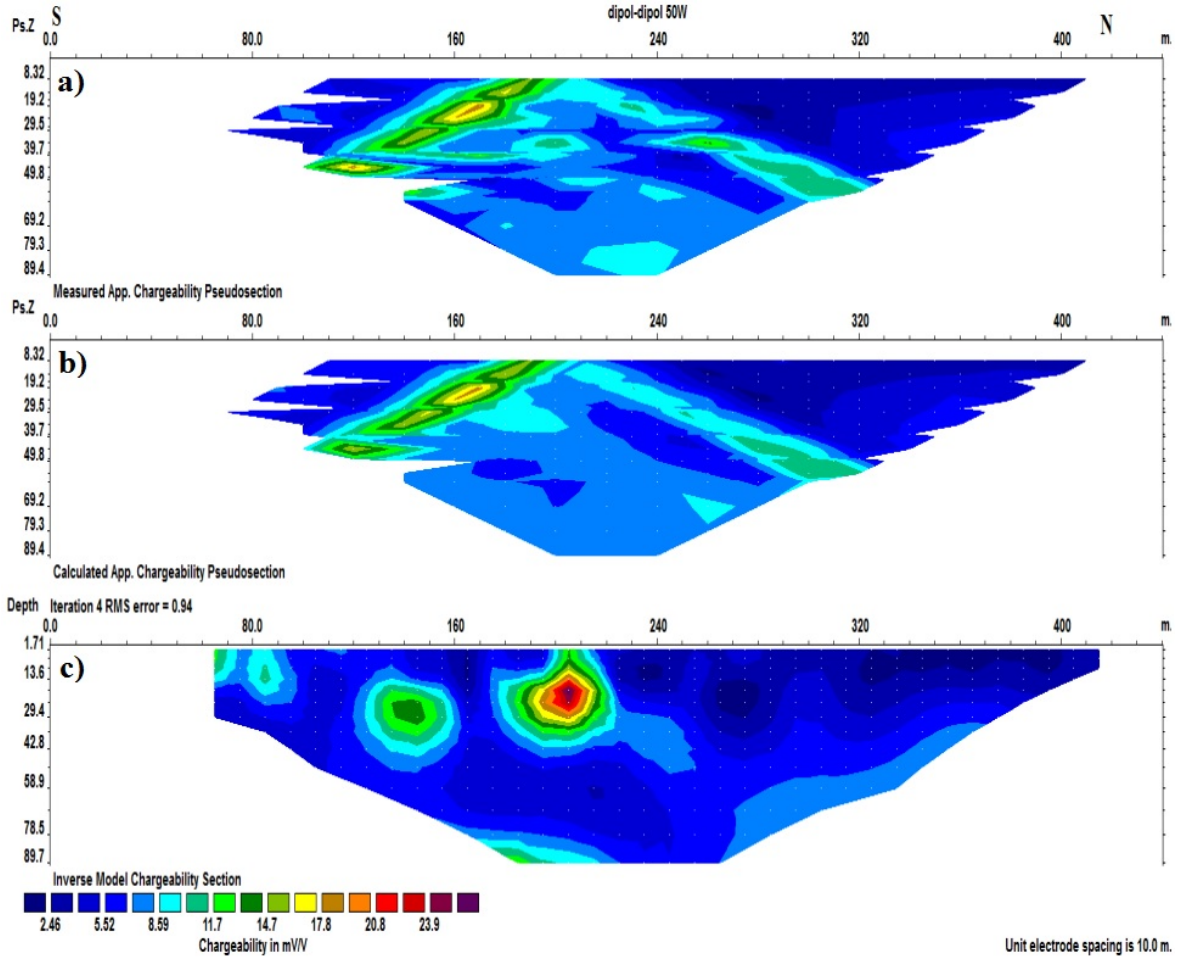


**Figure 6. Pseudo-sections and section of IP of inverse modeling of profile DD50W a) Pseudo-section of the measured data, b) Pseudo-section of the calculated data, c) Section of the inverse modeling.**

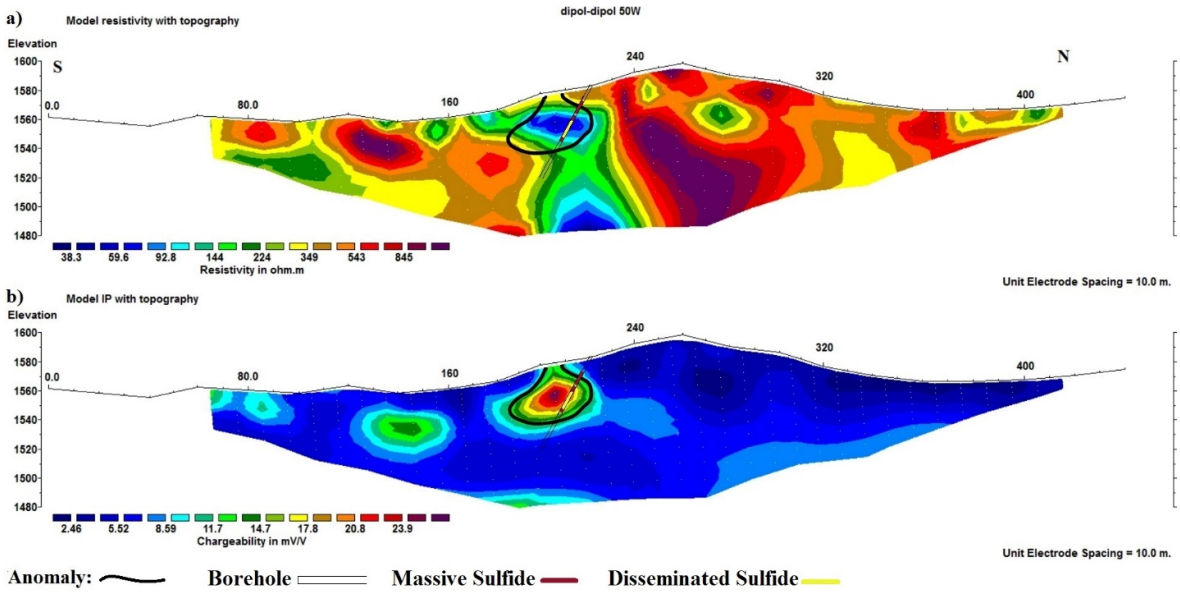


**Figure 7. Results of inverse modeling of the resistivity and IP data along survey line DD50W by applying topographic correction on the survey line (a) Electrical resistivity cross-section and (b) chargeability cross-section.**

On the promising area 2, the resistivity and IP data using the dipole-dipole array with electrode separations of 20 m and 40 m and steps of 20 m were made along the survey line DD450E. Figures 8 and 9 demonstrate the pseudo-sections and section of resistivity and IP of inverse modeling of the profile DD450E and the RMS error and iteration number for each model. Figure 10 shows the results of the inverse modeling of the resistivity and IP data along the survey line DD50W by applying a topographic correction on the survey line. According to Figure 10, an anomaly with a relatively high chargeability and a relatively low electrical resistivity is observed along this survey line. The chargeability intensity of this anomaly is greater from station 180 m to station 220 m, and the electrical resistivity is particularly low below these stations. This may be due to the higher grade of mineralization or higher intensity of mineralization. The disseminated and massive sulfide mineralization types were confirmed from the drilling information in this area. The massive sulfide mineralization corresponds to the region of low electrical resistivity.

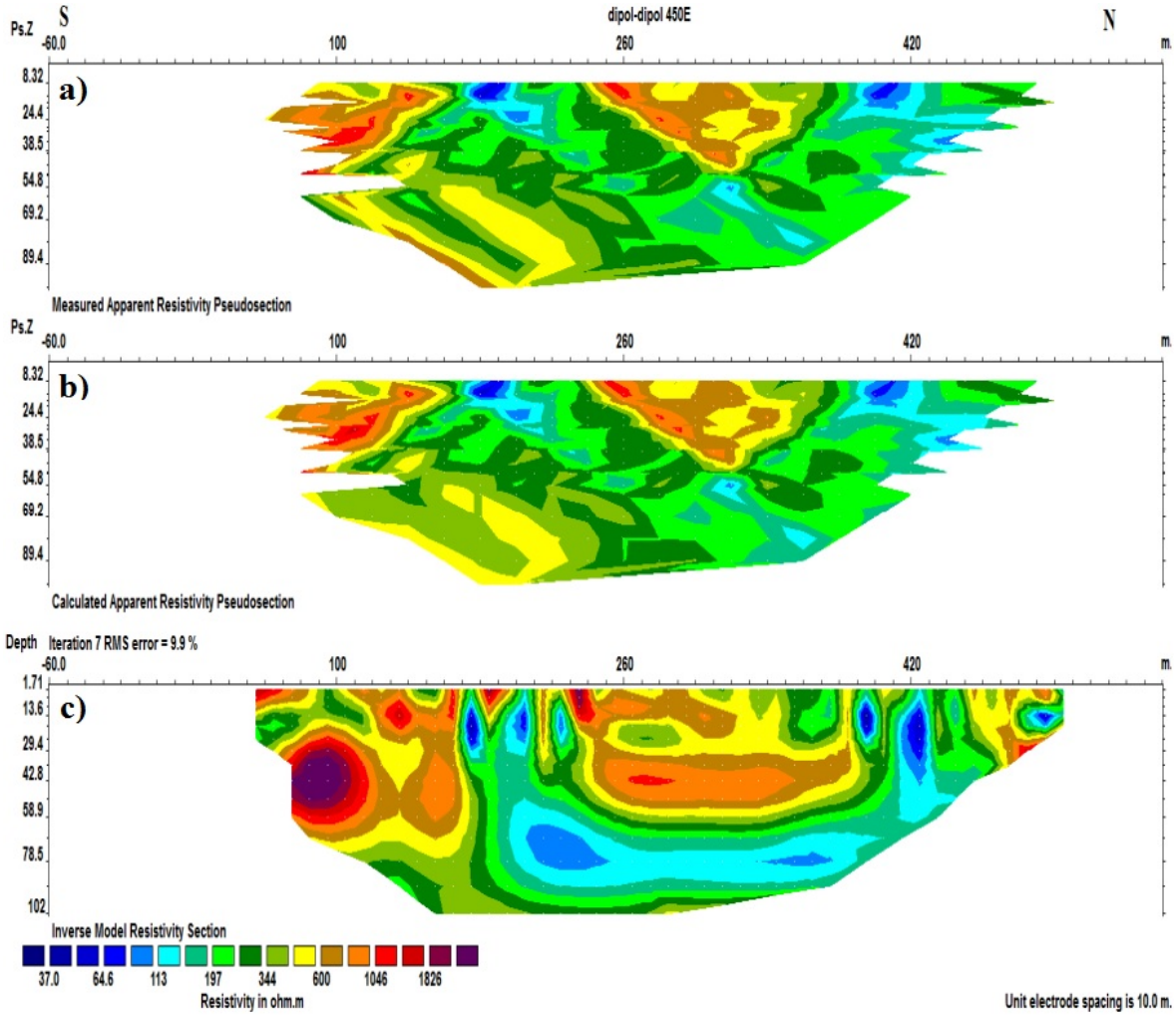


**Figure 8. Pseudo-sections and section of resistivity of inverse modeling of profile DD450E a) Pseudo-section of the measured data, b) Pseudo-section of the calculated data, c) Section of the inverse modeling.**

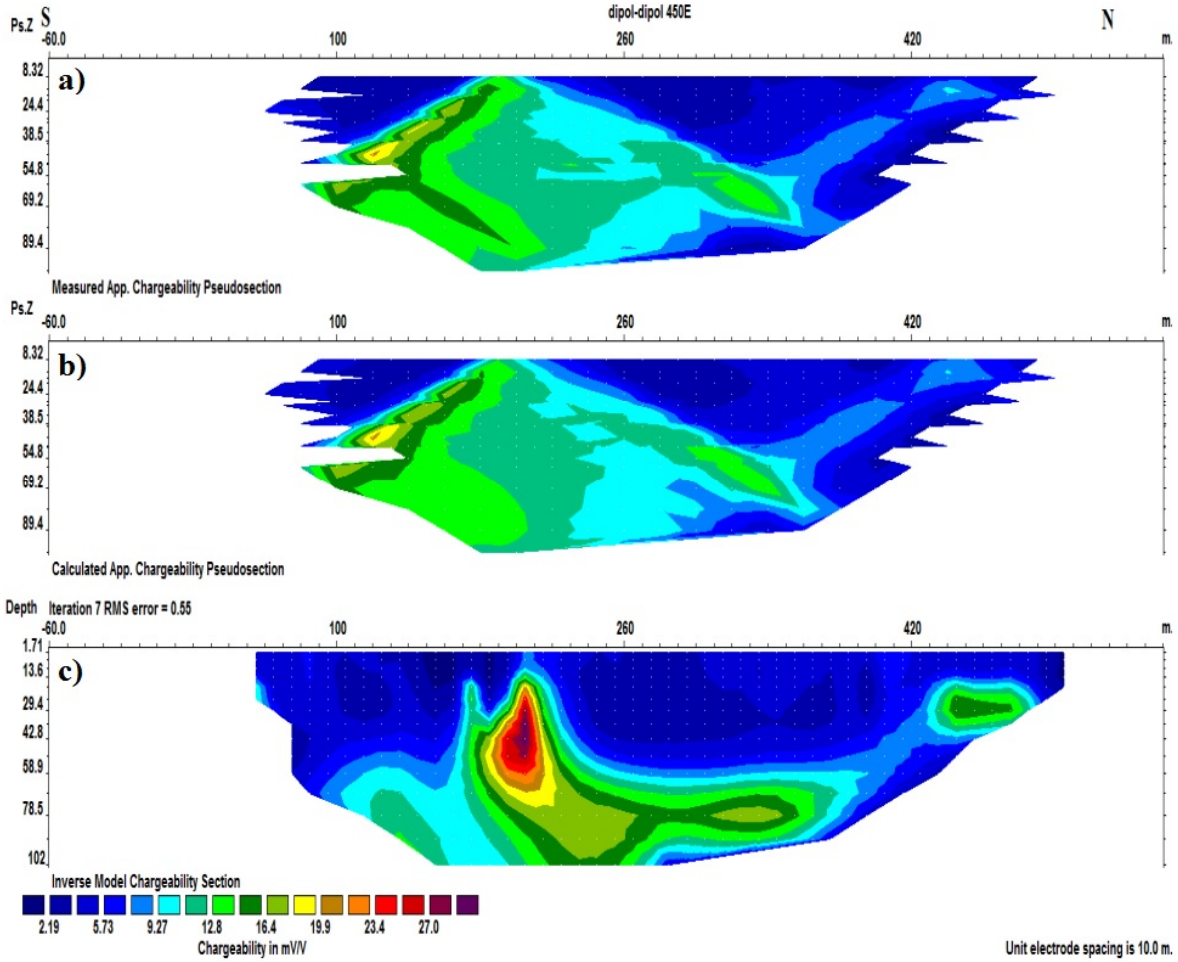


**Figure 9. Pseudo-sections and section of IP of inverse modeling of profile DD450E a) Pseudo-section of the measured data, b) Pseudo-section of the calculated data, c) Section of the inverse modeling.**

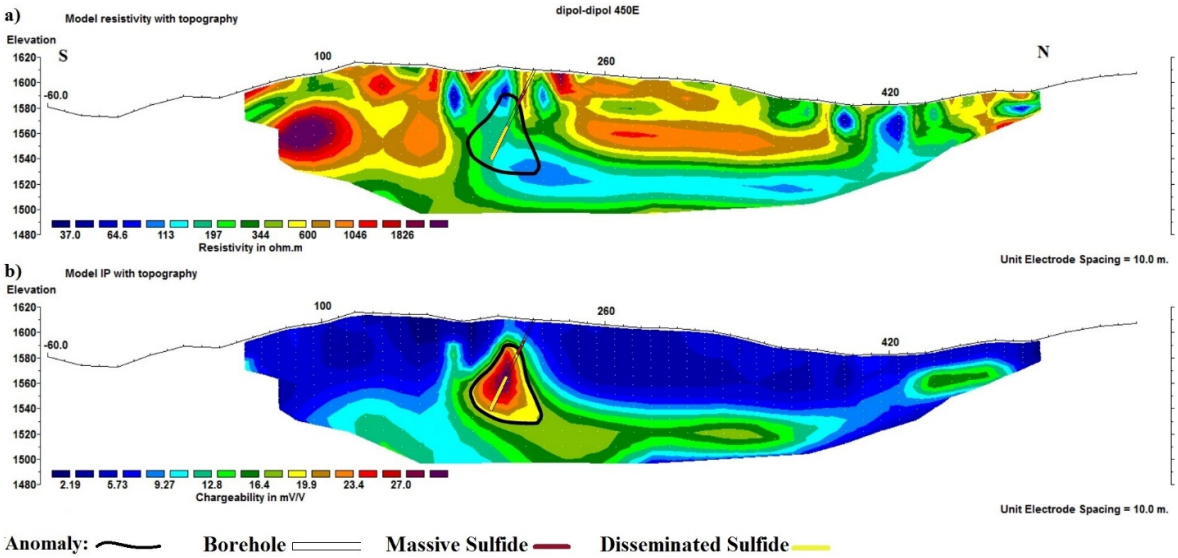


**Figure 10. Results of inverse modeling of the resistivity and IP data along the survey line DD450E by applying topographic correction on the survey line (a) Electrical resistivity cross-section and (b) Chargeability cross-section.**

The resistivity and IP measurements were carried out along the survey line DD600E using the dipole-dipole array with the electrode separations of 20 m and 40 m and steps of 20 m in order to investigate the sub-surface anomalies at the promising area 3. Figures 11 and 12 show the pseudo-sections and section of resistivity and IP of inverse modeling of the profile DD600E and the RMS error and iteration number for each model. In Figure 13, the results of inverse modeling of the resistivity and IP data along the survey line DD600E by applying the topographic correction on the survey line are shown. As it can be seen from the resistivity and IP cross-sections shown in Figure 13, the regions with high chargeability areas correspond to those of low to medium electrical resistivity areas. There are also two anomalies in these cross-sections. A minor anomaly that persists between stations 220 m and 240 m and an approximate depth of 30 m is related to the in-depth investigations of the promising area 2. The anomalies observed between the stations 230 m and 290 m and extended from the depth of about 50 m to deeper parts are also related to the in-depth investigations of thye promising area 3. Two mineralization types are observed in this promising area. The relatively high electrical resistivity sub-surface zones are due to the disseminated sulfide mineralization type, and the low electrical resistivity sub-surface zones are due to the massive sulfide mineralization type. Considering the significant presence of iron and copper sulfides in this area, a high potential of Fe and Cu mineralization exists in the area.

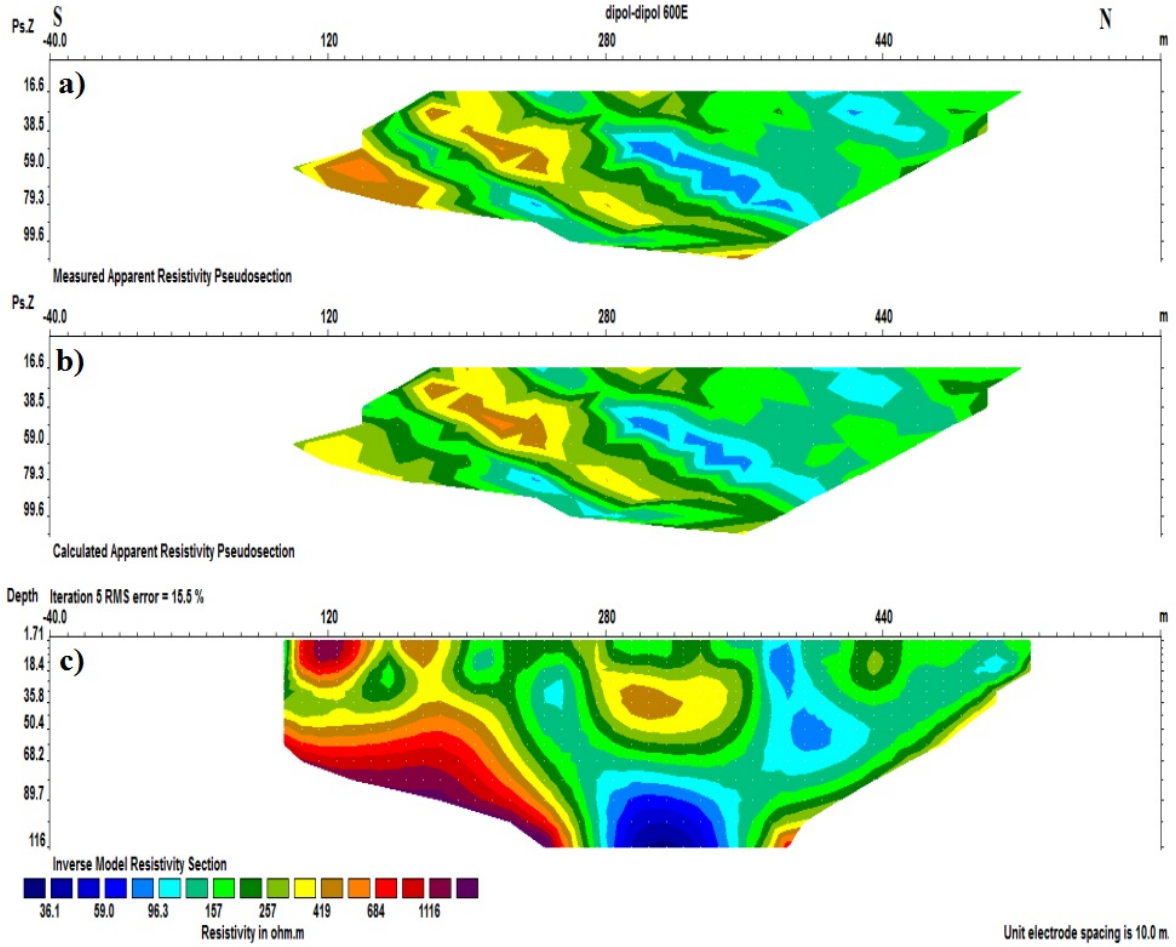


**Figure 11. Pseudo-sections and section of resistivity of inverse modeling of profile DD600E a) Pseudo-section of the measured data, b) Pseudo-section of the calculated data, c) Section of the inverse modeling.**

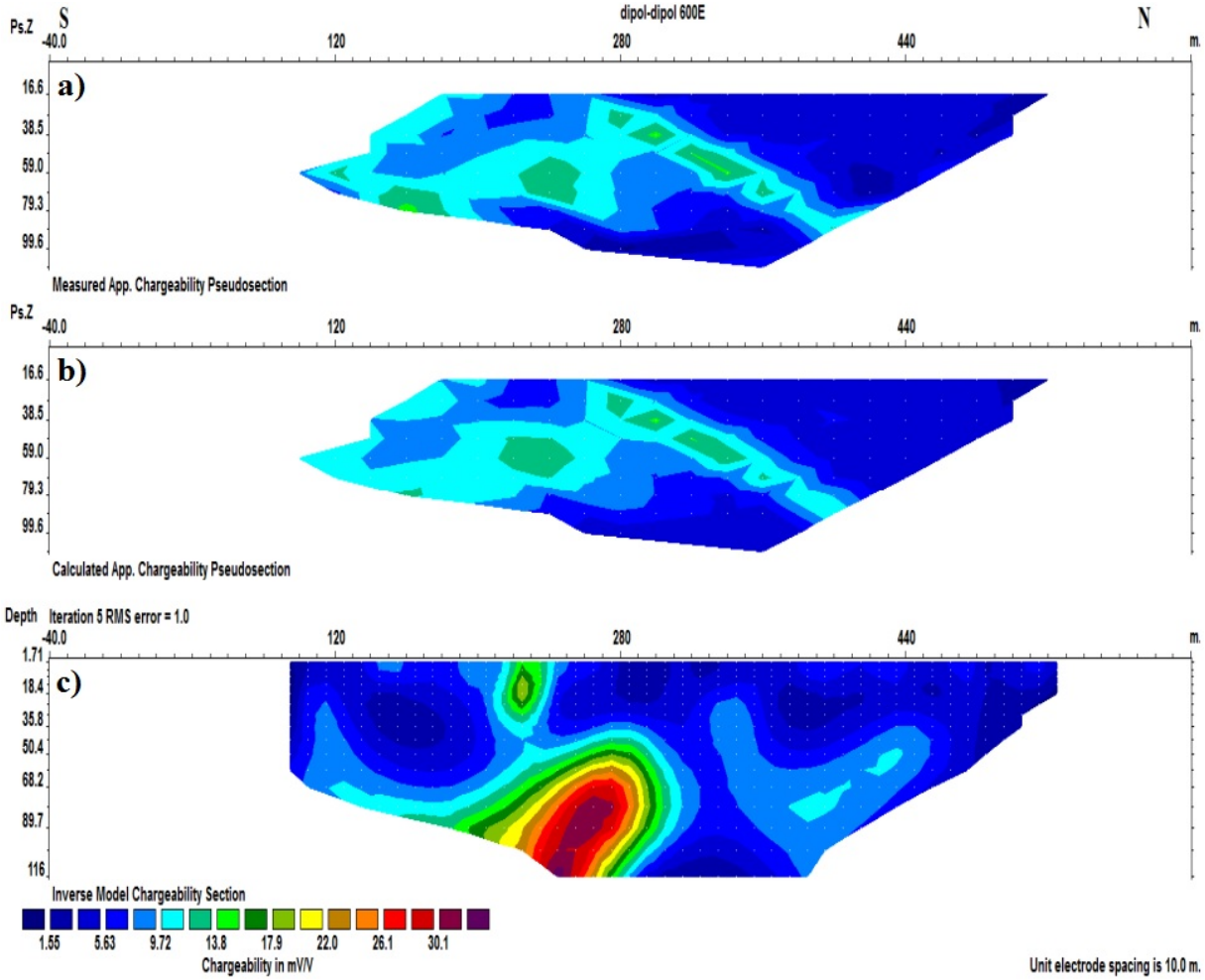


**Figure 12. Pseudo-sections and section of IP of inverse modeling of profile DD600E a) Pseudo-section of the measured data, b) Pseudo-section of the calculated data, c) Section of the inverse modeling.**

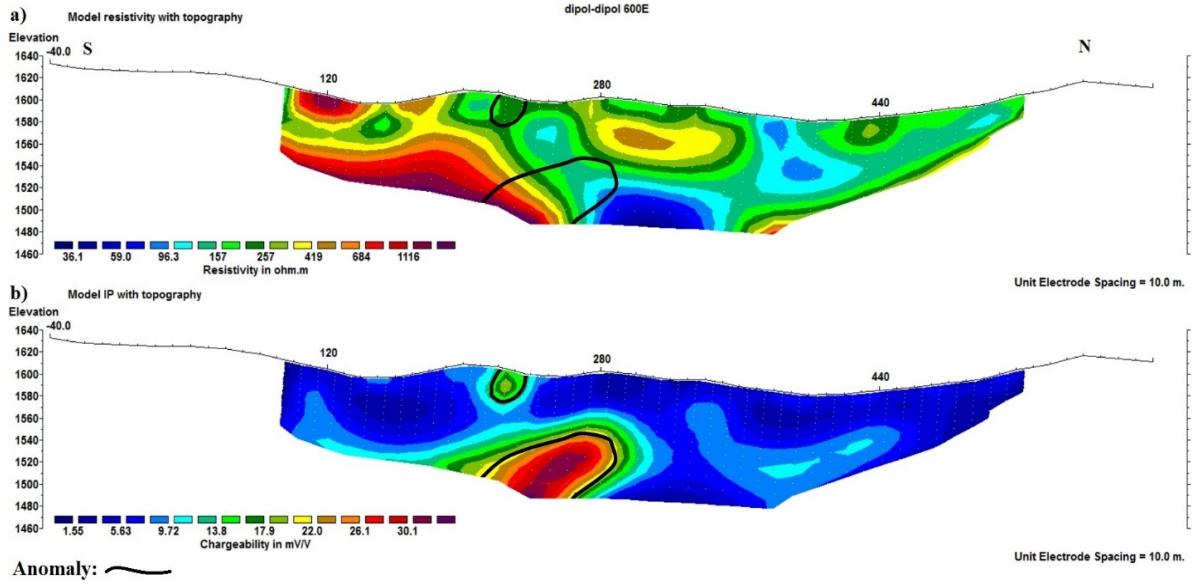


**Figure 13. Results of inverse modeling of the resistivity and IP data along the survey line DD600E by applying a topographic correction on the survey line (a) Electrical resistivity cross-section and (b) Chargeability cross-section.**

### 3.3. 3D resistivity and IP modeling

In general, the sub-surface geology of interest has a 3D resistivity distribution. Normally, this would require a 3D resistivity survey [17]. Therefore, the 3D modeling and representation of the geophysical data are very useful for achieving a general view of the anomalous areas. For this purpose, in order to map the mineralization distribution in detail, the 3D modeling of the electrical resistivity and IP data was performed. Figures 14 and 15 show the results of the 3D electrical resistivity and the IP modeling, respectively.

According to Figure 15, a slight anomaly can be seen from the surface to a depth of 7 m. From the depth of 7 m to 15 m and in the middle of this image, there is an evidence of mineralization that has a high electrical resistivity, as Figure 14 indicates. This anomaly continues in the higher depths, and has the highest IP values at depths of 47 m to 61 m, which corresponds to the medium electrical resistivity, and at the depths greater than 61 m, the IP intensity of this anomaly decreases. These areas can be attributed to the sulfide mineralization. Apart from these two anomalies, another anomaly can be seen in the third image related to the depths of 15.1 m to 24.3 m. This anomaly has its maximum values in the fourth image that is for the depths of 24.3 m to 35.0 m, and expands as it goes deeper. Moreover, the electrical resistivity of this anomaly is low, as observed in Figure 14.

Figures 16 and 17 demonstrate the 3D view of the results of the 3D modeling of the electrical resistivity and IP data, respectively, which have been acquired using the dipole-dipole array along various survey lines in the studied area having the displayed ground topography. As shown in these figures, the low electrical resistivity and high IP values are shown more specifically to represent the spatial distribution of mineralization beneath the ground surface. In addition to the 3D view of the mineralization, the drilling locations and topography of the studied area have also been shown for a better visualization of the area. The 3D irregular model with IP values above 15 mV/V is shown in Figure 17. This 3D model is roughly equivalent to the 3D model with low electrical resistivity values that is shown in Figure 16. The 3D model shown in Figures 16 and 17 demonstrates the distribution of the sulfide mineralization very well.

## 4. Conclusions

Investigation of the studied area with the help of the electrical resistivity and IP data obtained using the rectangle array led to the identification of the promising areas inside the studied area. For the in-depth investigations of the promising areas, the resistivity and IP data obtained using the dipole-dipole array were modeled. As a result of the inverse modeling of the resistivity and IP data using the dipole-dipole array, the resistivity and IP cross-sections were obtained, in which the geophysical anomalies associated with the sulfide mineralization zones were identified. This mineralization was confirmed by the geological evidence in the area. The drilling operations were also carried out at some points in the studied area in order to confirm the mineralization. The performed 3D resistivity and IP modeling also showed the mineralization areas. A 3D representation of the electrical resistivity and IP data modeling contributed to a better view of the spatial distribution of the sulfide mineralization.

As a result of this research work, we observed that the application of the electrical resistivity and IP data using the rectangle array was successful in prospecting the polymetallic deposit in the area. Moreover, we observed that the simultaneous use of both the electrical resistivity and IP methods with employing the dipole-dipole array was very convenient and reliable for the in-depth investigations of the promising polymetallic zones. Applying these methods for the in-depth investigations resulted in a cost-effective, time-saving, and consistent image of sub-surface mineralization. These geophysical methods also had a less environmental impact than the drilling methods. By comparing the results obtained from these two methods in the anomalous regions, one can obtain information on the grade and type of mineralization (i.e. disseminated or massive mineralization). By combining the geophysical and geological results in exploring the polymetallic deposits, the best drilling points can be suggested. In most of the cross-sections obtained from the inverse modeling of the resistivity and IP data, it was seen that the mineralization areas had a high chargeability and a low to medium electrical resistivity, indicating the presence of sulfide mineralization in the sub-surface. The drilling operations carried out along the survey lines confirmed the identified anomalies. Since all the structures are in the form of 3D in nature, the 3D modeling of the resistivity and IP data can give a better picture of the sub-surface structures. The 3D

representation of the modeling results can also give a better and more understandable spatial distribution of the mineralization zones.

Due to the presence of schists in this area and the presence of clay minerals in the schists, these structures, similar to mineralization, exhibit a relatively low electrical resistivity and a relatively high chargeability, and therefore, act as noise sources in the geophysical identification of the sulfide mineralization. In the cases where these rocks are also associated with poor mineralization, they show a high chargeability (even more than the mineralization zones). The use of the spectral IP (SIP) method to separate the metallic minerals from the non-metallic ones (e.g. clays) is suggested.

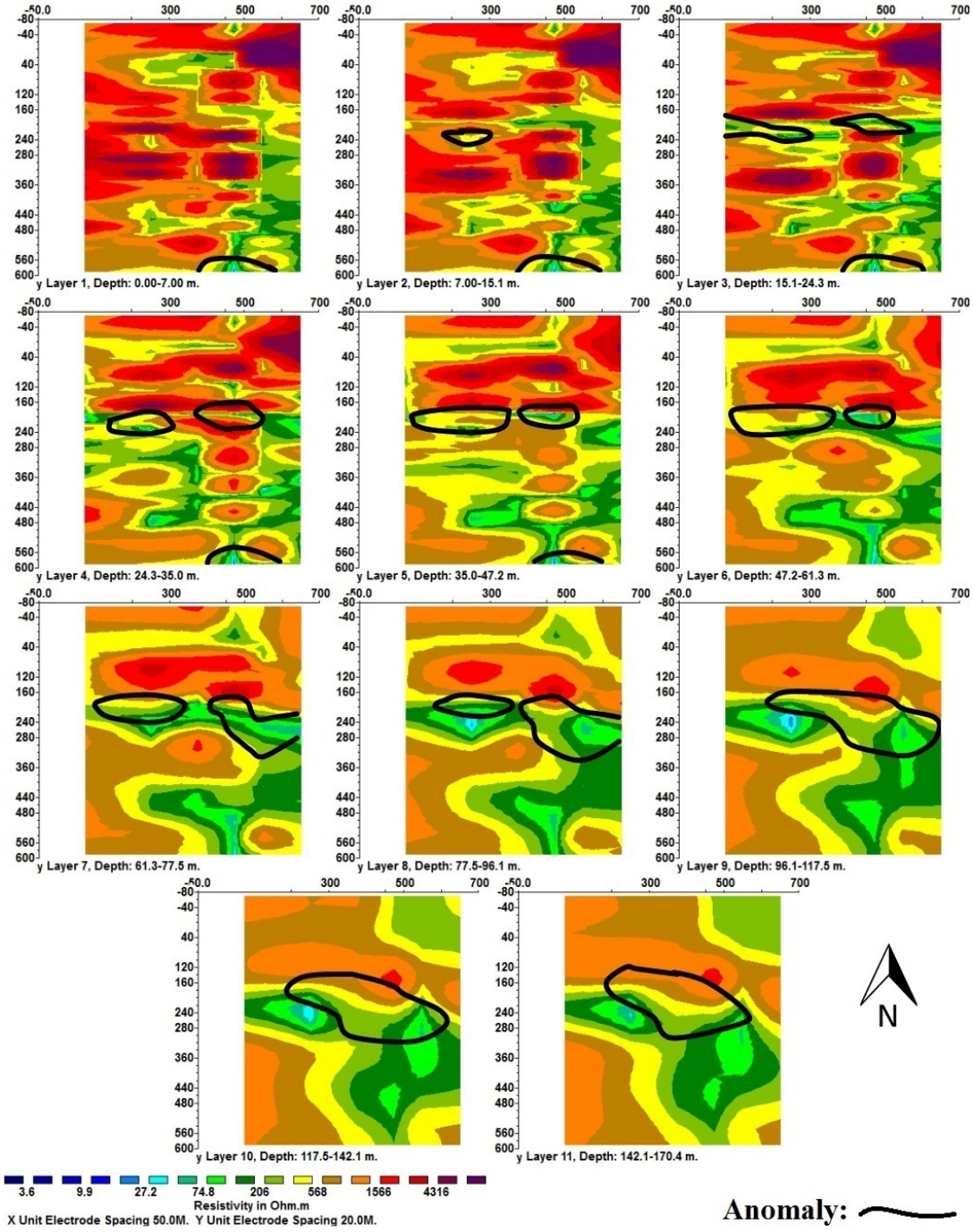


**Figure 14. 3D modeling results of the electrical resistivity data acquired using the dipole-dipole array along various survey lines in the studied area.**

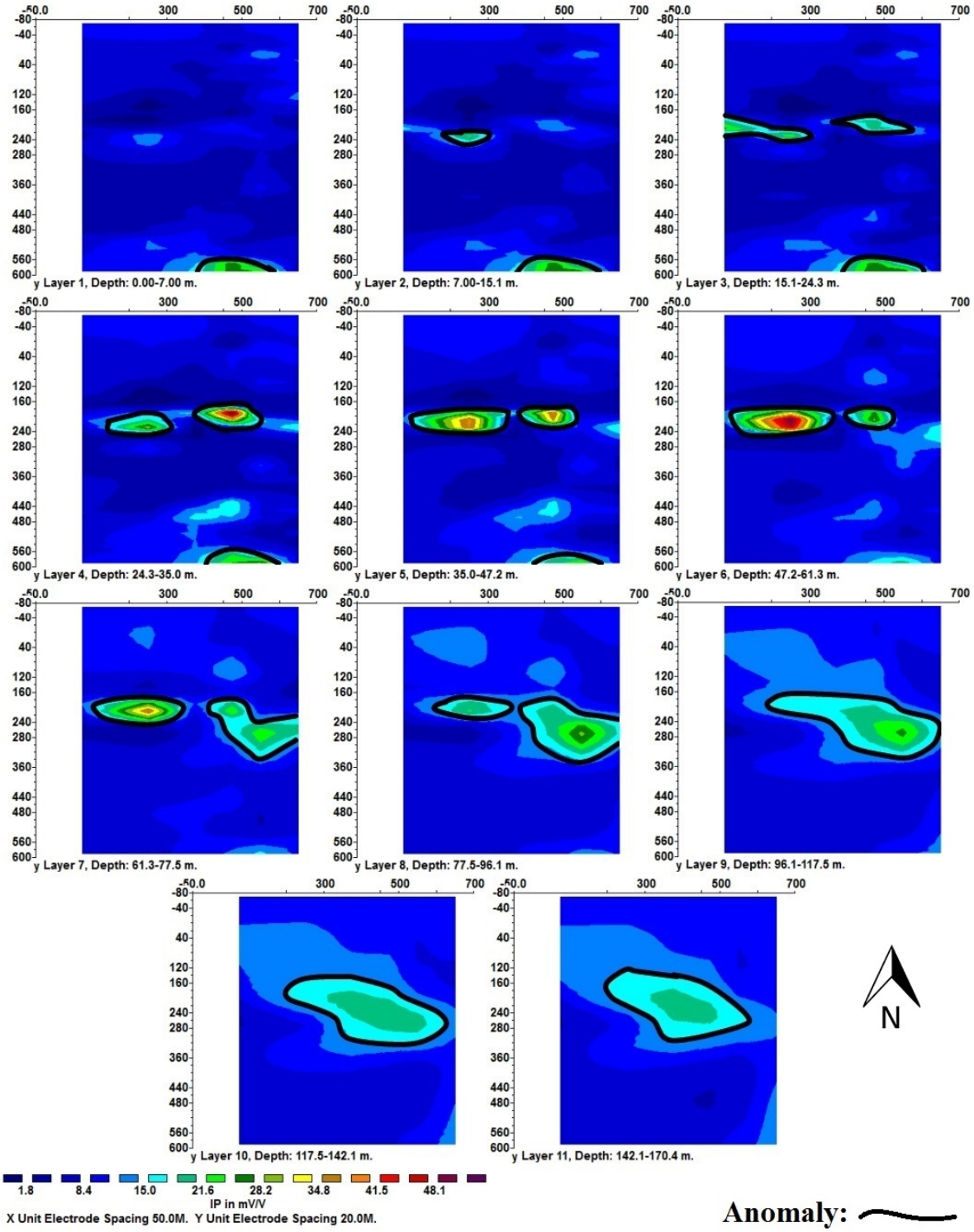


**Figure 15. 3D modeling results of the IP data acquired using the dipole-dipole array along various survey lines in the studied area.**

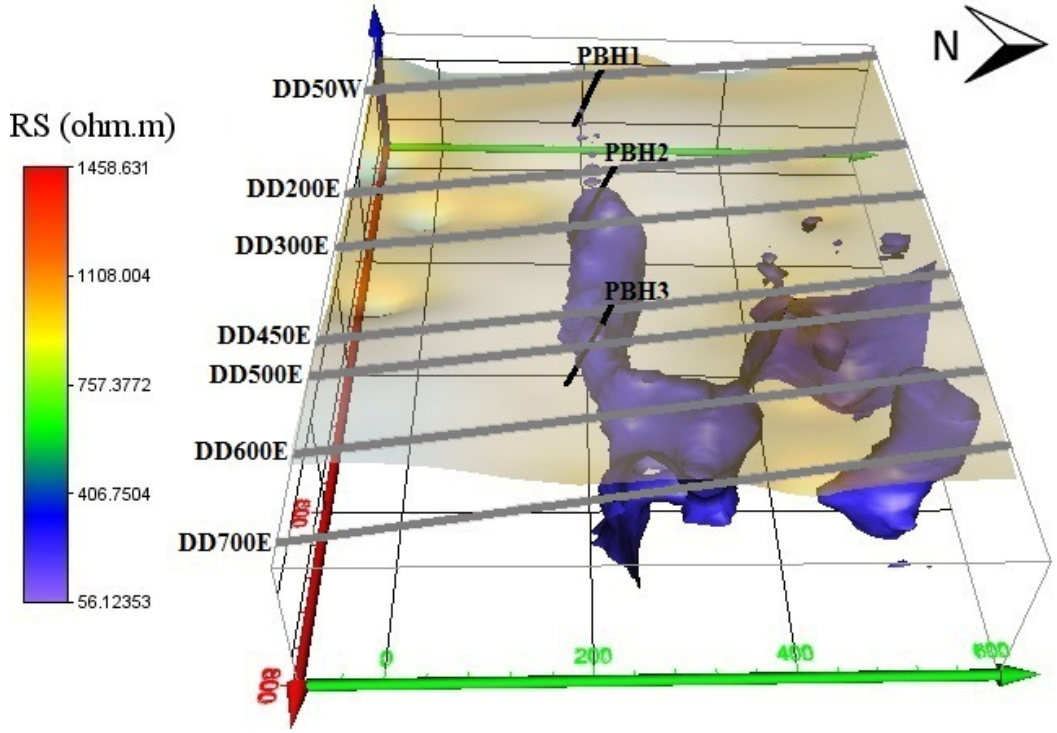


**Figure 16. 3D representation of the results of 3D modeling of the electrical resistivity data acquired using the dipole-dipole array along various survey lines in the studied area in which the topography of the area has also been considered.**

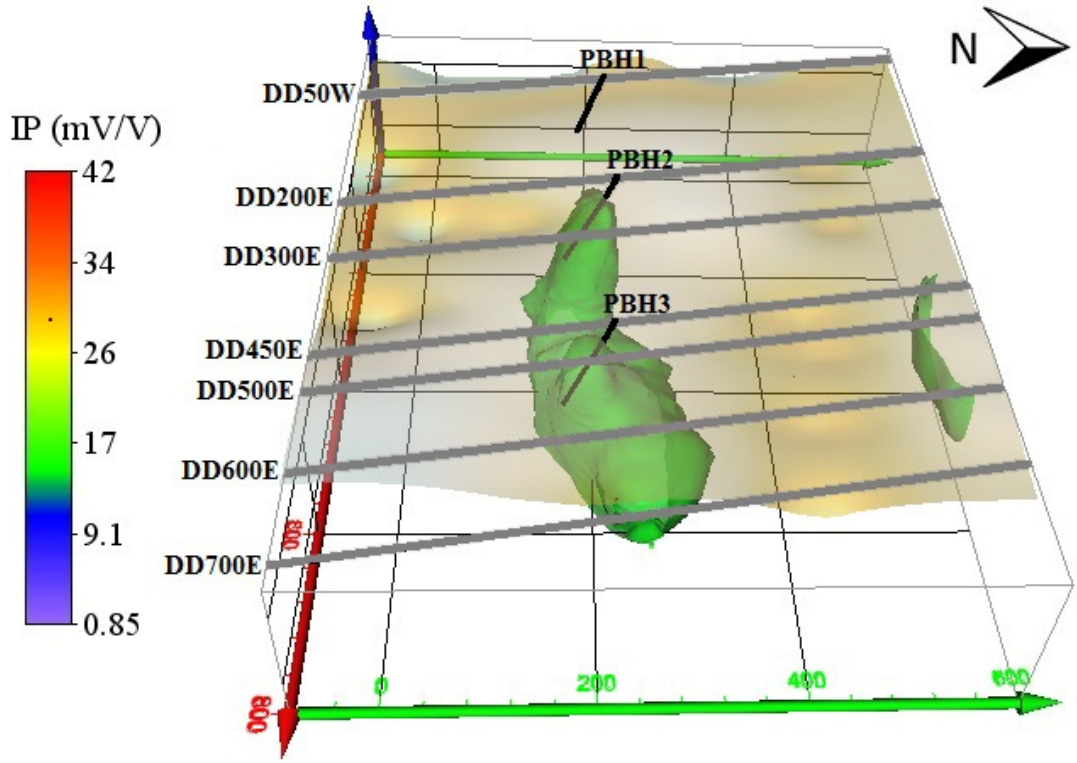


**Figure 17. 3D representation of the results of 3D modeling of the IP data acquired using the dipole-dipole array along various survey lines in the studied area in which the topography of the area has also been considered.**

## References

[1]. Abdulsamad, F., Revil, A., Ahmed, A.S., Coperey, A., Karaoulis, M., Nicaise, S. and Peyras, L. (2019). Induced polarization tomography applied to the detection and the monitoring of leaks in embankments. Engineering Geology, 254: 89-101.

[2]. Aizebeokhai, A.P. (2009). Geoelectrical resistivity imaging in environmental studies. In Appropriate Technologies for Environmental Protection in the Developing World (pp. 297-305). Springer, Dordrecht.

[3]. Deceuster, J. and Kaufmann, O. (2012). Improving the delineation of hydrocarbon-impacted soils and water through induced polarization tomographies: A field study at an industrial waste land. Journal of Contaminant Hydrology, 136, 25-42.

[4]. Di Maio, R., Fais, S., Ligas, P., Piegari, E., Raga, R. and Cossu, R. (2018). 3D geophysical imaging for site-specific characterization plan of an old landfill. Waste Management, 76: 629-642.

[5]. Eftekharnezhad, J., Hamzehpour, B., Aghanabati, A. and Baroyant, V. (1976). Geological map of Kashmar, 1:250000 scale. Geological Survey of Iran, Tehran, Iran.

[6]. Gallistl, J., Weigand, M., Stumvoll, M., Ottowitz, D., Glade, T. and Orozco, A.F. (2018). Delineation of sub-surface variability in clay-rich landslides through spectral induced polarization imaging and electromagnetic methods. Engineering geology. 245: 292-308.

[7]. Gazoty, A., Fiandaca, G., Pedersen, J., Auken, E., Christiansen, A.V. and Pedersen, J.K. (2012). Application of time domain-induced polarization to the mapping of litho-types in a landfill site. Hydrology and Earth System Sciences. 16 (6): 1793-1804.

[8]. Goad, R.E., Mumin, A.H., Duke, N.A., Neale, K.L., Mulligan, D.L. and Camier, W.J. (2000). The NICO and Sue-Dianne Proterozoic, iron oxide-hosted, polymetallic deposits, Northwest Territories: Application of the Olympic Dam model in exploration. Exploration and Mining Geology. 9 (2): 123-140.

[9]. Google Earth Pro 7.3.3.7786 (32-bit). (July 21, 2020). Kaboudan area, Razavi Khorasan Province, Iran. 40 S 588898.00 m E 3920760.45 m N, Eye alt 2.51 Km. <http://www.google.com/earth/index.html> (Accessed August 20, 2020).

[10]. Gurin, G., Tarasov, A., Ilyin, Y. and Titov, K. (2013). Time-domain spectral-induced polarization of disseminated electronic conductors: Laboratory data analysis through the Debye decomposition approach. Journal of Applied Geophysics. 98: 44-53.

[11]. Gurin, G.V., Tarasov, A.V., Il'in, Y.T. and Titov, K.V. (2017). Transient characteristics of induced polarization in inhomogeneous media (from results of 2D numerical simulation). Russian Geology and Geophysics. 58 (5): 624-634.

[12]. Heritiana, A.R., Riva, R., Ralay, R. and Boni, R. (2019). Evaluation of flake graphite ore using self-potential, electrical resistivity tomography (ERT) and induced polarization methods in east coast of Madagascar. Journal of Applied Geophysics.

[13]. Hördt, A., Blaschek, R., Kemna, A. and Zisser, N. (2007). Hydraulic conductivity estimation from induced polarisation data at the field scale—the Krauthausen case history. Journal of Applied Geophysics. 62 (1): 33-46.

[14]. Karimpour, M. (2010). Taknar massive sulfide, U-Pb zircon geochemistry and Sr-Nd isotopic characteristic of Bornaward granitoids, Iran. 18th symposium of crystallography and mineralogy of Iran. Tabriz, Iran.

[15]. Kearey, P., Brooks, M. and Hill, I. (2013). An introduction to geophysical exploration. John Wiley and Sons.

[16]. Kirsch, R. (2006). Groundwater geophysics (Vol. 493). Berlin: Springer.

[17]. Knödel, K., Lange, G. and Voigt, H.J. (2007). Environmental geology: handbook of field methods and case studies. Springer Science & Business Media.

[18]. Loke, M.H. (2010). Tutorial: RES2DINV ver. 3.59, Rapid 2-D Resistivity & IP inversion using the least-squares method. Malaysia, Geotomo Software.

[19]. Mary, B., Saracco, G., Peyras, L., Vennetier, M., Mériaux, P. and Camerlynck, C. (2016). Mapping tree root system in dikes using induced polarization: Focus on the influence of soil water content. Journal of Applied Geophysics. 135: 387-396.

[20]. Pelton, W.H., Ward, S.H., Hallof, P.G., Sill, W.R. and Nelson, P.H. (1978). Mineral discrimination and removal of inductive coupling with multifrequency IP. Geophysics. 43 (3): 588-609.

[21]. Qi, Y., El-Kaliouby, H., Revil, A., Ahmed, A. S., Ghorbani, A. and Li, J. (2019). 3D modeling of frequency-and time-domain electromagnetic methods with induced polarization effects. Computers & geosciences. 124: 85-92.

[22]. Revil, A., Qi, Y., Ghorbani, A., Ahmed, A.S., Ricci, T. and Labazuy, P. (2018). Electrical conductivity and induced polarization investigations at Krafla volcano, Iceland. Journal of Volcanology and Geothermal Research. 368: 73-90.

[23]. Safari, M. (2009). Prospecting report of 1:25000 Kaboudan (Bardeskan area). Geological Survey of Iran, Tehran, Iran.

[24]. Safari, M. (2010). Introducing new mineralization of massive sulfide deposits in Kaboudan area (north of Bardeskan) using feature analysis method and element

carat maps. 1st Conference of Iranian Society of Economic Geology. Mashhad, Iran.

[25]. Safari, M. and Akbari-moghadam, M. (2011). Exploration of massive sulfide deposits in Kaboudan area, north of Bardeskan. 29th National Geosciences Congress, Geological Survey of Iran, Tehran, Iran.

[26]. Selley, R.C., Cocks, R. and Plimer, I. (2004). Encyclopedia of geology. Academic Press.

[27]. Shahrabi, M., Hosseini, K., Shabani, K., Massomi, R. and Haddadan, M., (2006). Geological map of Bardaskan, 1:100000 scale. Geological Survey of Iran, Tehran, Iran.

[28]. Shao, Z., Revil, A., Mao, D. and Wang, D. (2018). Finding buried metallic pipes using a non-destructive approach based on 3D time-domain induced polarization data. Journal of Applied Geophysics. 151: 234-245.

[29]. Veeken, P.C., Legeydo, P.J., Davidenko, Y.A., Kudryavceva, E.O., Ivanov, S.A. and Chuvaev, A. (2009). Benefits of the induced polarization geo-electric method to hydrocarbon exploration. Geophysics. 74 (2): B47-B59.

[30]. White, R.M.S., Collins, S. and Loke, M.H. (2003). Resistivity and IP arrays, optimized for data collection and inversion. Exploration Geophysics. 34 (4): 229-232.

# مدل‌سازی داده‌های پلاریزاسیون القایی (IP) و مقاومت‌ویژه به منظور پی‌جویی و اکتشاف ذخایر پلی‌متال در منطقه کبودان، شرق ایران

**فرزانه جمالی، علیرضا عرب‌امیری*، ابوالقاسم کامکارروحانی و علی بهرامی**

**دانشکده مهندسی معدن، نفت و ژئوفیزیک، دانشگاه صنعتی شاهرود، شاهرود، ایران**

ارسال ۲۰۲۰/۱۲/۱۲، پذیرش ۲۰۲۱/۰۶/۱۱

* نویسنده مسئول مکاتبات: alirezaarabamiri@yahoo.com

**چکیده:**

در اکتشافات ژئوفیزیکی رسیدن به تصویری دقیق از ویژگی‌های زیرسطحی، هدف برداشت است. به منظور دست‌یابی به این امر، عملیات ژئوفیزیکی مقاومت‌ویژه الکتریکی و قطبش القایی (IP) برای اکتشاف محل‌های کانی‌سازی سولفیدی زیرسطحی انجام می‌گیرد. با توجه به شواهد کانی‌سازی در منطقه کبودان واقع در شهرستان بردسکن، ابتدا پی‌جویی ذخایر پلی‌متال به روش مقاومت‌ویژه الکتریکی و IP با آرایه مستطیلی انجام شده است. سپس برای اکتشاف بی‌هنجاری‌های تعیین شده و مناطق مستعد کانی‌سازی، مقاطع دوبعدی تهیه و به کمک اطلاعات زمین‌شناسی مورد تفسیر قرار گرفته است؛ که این برداشتهای ژئوفیزیکی منجر به آشکارسازی چند ناحیه مستعد کانی‌سازی گردید. سپس به منظور دست‌یابی به تصویری دقیق از کانی‌سازی زیرسطحی و دید کلی از توزیع کانی‌سازی در عمق، مدل‌سازی سه‌بعدی داده‌های برداشت شده صورت گرفته است و نتایج حاصل از این مدل‌سازی به نمایش در آمده است. نواحی کانه‌زا در اکثر مناطق با بارپذیری بالا و همچنین مقاومت‌ویژه پایین تا متوسط شناسایی می‌شود؛ که این امر را می‌توان به کانی‌سازی فلزی و حضور کانی‌های سولفیدی در مناطق کانی‌سازی نسبت داد. کانی‌سازی در بسیاری از این نواحی با روند تقریبی شرقی-غربی و همچنین با شدت‌های متفاوت مقاومت‌ویژه و IP مشخص است. اطلاعات زمین‌شناسی و حفاری‌های صورت گرفته در این منطقه، تفسیرهای انجام شده را تأیید می‌کند.

**کلمات کلیدی:** قطبش القایی، مقاومت‌ویژه الکتریکی، ذخایر پلی‌متال، مدل‌سازی سه بعدی، آرایه مستطیلی، آرایه دوقطبی-دوقطبی، بارپذیری.